Design and construction of the Artificial Patient module for testing bioimpedance measuring devices

Marcel Młyńczak [a], Katarzyna Pariaszewska [a], Wiktor Niewiadomski [b], Gerard Cybulski* [a,b]
[a] Institute of Precision and Biomedical Engineering, Faculty of Mechatronics, Warsaw University of Technology, ul. św. Andrzeja Boboli 8, 02-525 Warsaw, POLAND
[b] Department of Applied Physiology, Mossakowski Medical Research Centre, Polish Academy of Sciences, ul. Pawińskiego 5, 02-106 Warsaw, POLAND

* *G.Cybulski@mchtr.pw.edu.pl*

ABSTRACT

The purpose of this study was to describe the design of the electronic module for testing bioimpedance measuring devices, for example impedance cardiographs or impedance pneumographs. Artificial Patient was conceived as an electronic equivalent of the impedance of skin-electrode interface and the impedance between electrodes – measured one. Different approaches in imitating a resistance of skin and an impedance of electrode-skin connection were presented.
The module was adapted for frequently applied tetrapolar electrode configuration. Therefore the design do not enclose the elements simulating impedance between skin and receiver electrodes due to negligible effect of this impedance on the current flow through the receiver.
The Artificial Patient enables testing either application generators, or receiver parts, particularly the level of noise and distortions of the signal. Use of digitally controlled potentiometer allows simulating different tissue resistances changes such as constant values, very-low-frequency and low-frequency changes corresponding to those caused by breathing or heart activity. Also it allows distorting signals in order to test algorithms of artifacts attenuation.

Keywords: Bioimpedance, Reocardiography, Reopneumography, Skin-Electrode Interface, Artificial Patient

1. INTRODUCTION

1.1 Impedance Reography

Bioimpedance measurements are used to record or monitor functions of cardiovascular system and lungs, as well as for thoracic fluid content and body composition measurements.

Depending on the electrode placement on the body (Fig.1) the signals obtained may be used to measure heart stroke volume [1], arterial blood flow in the limbs or lungs tidal volume [2,3].

Electrical impedance is usually measured with four electrodes (tetrapolar method), two driving, two receiving ones [4]. Excitation current (for example sinusoidal 100kHz 400μA) is flowing through driving electrodes and the tissues and the measured signal is voltage between receiving electrodes.

It is known that the tissue impedance is significantly smaller than the impedance of the connection of the electrode and the skin-electrode interface.

Photonics Applications in Astronomy, Communications, Industry, and High-Energy Physics Experiments 2013, edited by Ryszard S. Romaniuk, Proc. of SPIE Vol. 8903, 890314
 · doi: 10.1117/12.2031879

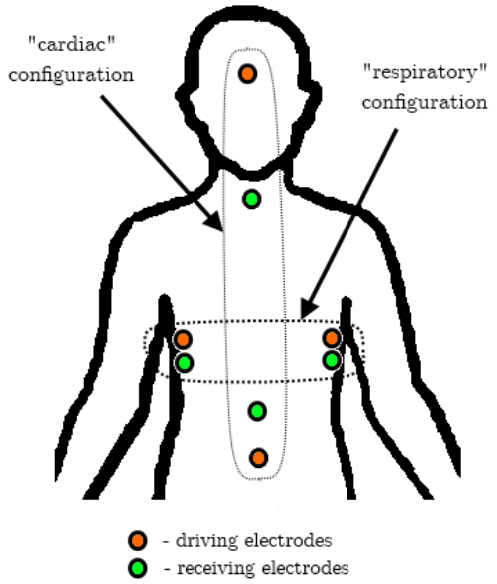

Figure 1. Electrode configuration in Reocardiography and Reopneumography [1,2]

1.2 Skin-electrode interface electrical equivalent

It has been observed that increase of excitation frequency causes decrease of total impedance [5,6]. This observation has been explained by the participation of capacitive components in the skin-electrode interface.

Three types of models have been proposed – single exponential dynamic model [7,8], double exponential dynamic model [7,8] and double exponential model with constant phase element [9] (Fig.2).

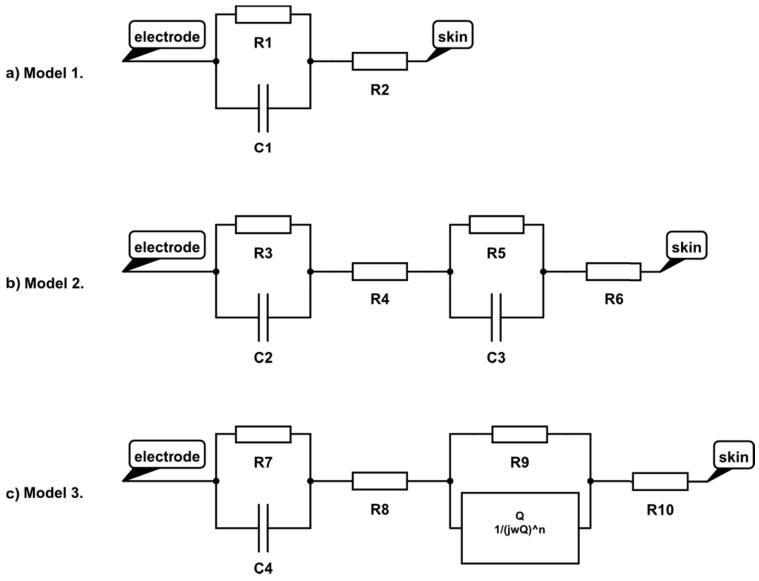

Figure 2. Types of skin-electrode interface models

Because of the difficulty of hardware implementation of Model 3. (Fig. 2c), only single and double exponential models will be considered as they could be constructed by electrical passive elements in simple way.

In first model, resistor R1 in parallel with capacitor C1 imitate the impedance of the barrier layer between the skin and electrode. Resistor R2 in series corresponds to resistive features of electrolyte (in Ag/AgCl electrodes) and subcutaneous layer and deeper tissues properties [6,10]. In second model, capacitive components (C2,C3) imitate electrode's permittivity and epidermal layer, respectively. Resistor R3 fulfills similar role as resistor R1 in first model, the same as resistors R4 and R6 with R2. Resistor R5 corresponds to stratum corneum layer [10].

Apart from the features above, wet Ag/AgCl electrodes may have greater impedance than dry ones [8]. On the other side, abrasion and moisturizing of the skin effect decrease of approximate impedance [6,11].

1.3 Models parameters identification

Model parameters can be obtained by passing the current through the tissue-electrode circuit, either by analyzing response to rectangular pulses [7], or by measuring magnitude and phase responses to the sinusoidal signals with different frequencies [8].

2. METHODOLOGY

2.1 Components selection

We calculated the magnitude and phase responses (Fig. 3) for Model 1. and 2. from Figure 2. of skin-electrode interface with parameters [8,12]:

$$R1 = 1M\Omega\,, R2 = 10k\Omega\,, R3 = 220k\Omega\,, R4 + R6 = 10k\Omega\,, R5 = 440k\Omega\,, C1 = 22nF\,, C2 = 6.6\mu F\,, C3 = 500nF$$

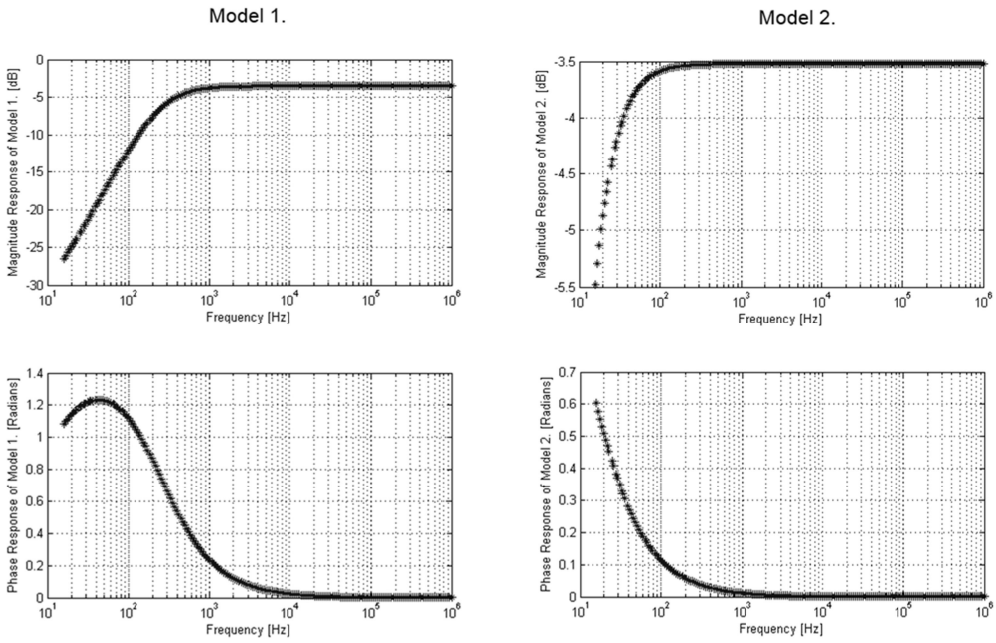

Figure 3. Magnitude and phase responses for Model 1. and 2. for R_{load} = 20kΩ

Assambo et al. [8,10] suggest that second model fits better to the empirical results, but as there are no differences between models for high frequencies, we have chosen the simpler, first one.

In order to produce small changes of tissue impedances with high precision we use parallel connection of two resistors, R_{const} and R_{var}. Dependence between R_{equiv} and R_{var} is clearly nonlinear, but we could use the range of values where this dependence remains firmly linear, as demonstrated in Figure 4.:

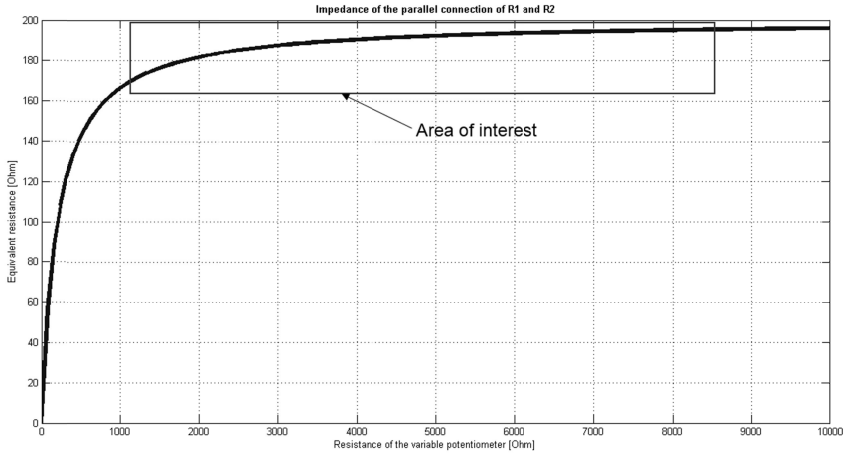

Figure 4. Impedance of the parallel connection of $R_{const} = 200\Omega$ and $R_{var} \in [0\Omega - 10k\Omega]$ with an area of interest

Using the two resistors circuit proposed above it is possible to reproduce typical situation where the constant value of tissue impedance is much greater than amplitude of variable component.

Of note, in the present design of Artificial Patient we neglected the capacitive component of tissue impedance.

2.2 Tetrapolar adaptation

As the input impedance of the bioimpedance measuring devices is very high, I_{bias} (Fig.5) is small in proportion to I_{excit}. Therefore we applied the electrical equivalent of the electrode-skin contact only for driving electrodes inputs.

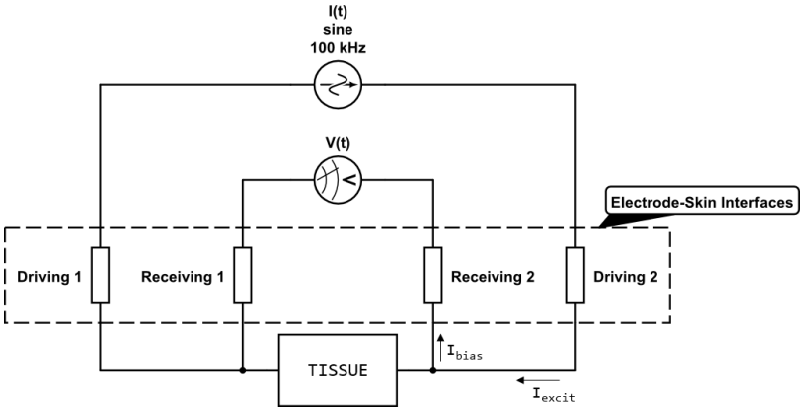

Figure 5. Assistance circuit for an explanation of tetrapolar adaptation

2.3 Design of the Artificial Patient

The Artificial Patient was designed as a connection of two circuits modeling electrode-skin interface according to single exponential dynamic model and two resistors circuit modeling tissue resistance. Electrode potentials are imitated by batteries as voltage sources in series with R2 resistor (see Fig.2a).

As R_{var} resistor is used digital potentiometer TPL0401a controlled by microcontroller MSP430G2452 via I^2C, both by Texas Instruments®.

The potentiometer used in construction had 10kΩ end-to-end resistance regulation options with 7-bit resolution. Potentiometer as well as microcontroller are supplied by 3 AA 1,2V rechargeable batteries. Bioimpedance measuring device is connected to the Artificial Patient using typical four electrode connectors, as shown in Figure 6.

Figure 6. The image of the PCB-mounted prototype of the Artificial Patient module

We used Artificial Patient with universal bioimpedance measuring device designed by us. The design of this device will be published elsewhere.

3. DATA

3.1 Application

We prepared a script in MATLAB® to produce the code for the microcontroller which changes the R_{var} in desired way taking into account the nonlinearities described in 2.1. We set R_{const} and signal shape according to the formula or as a vector of predetermined values. As a result we get plots of desired signal, signal produced by Artificial Patient model, programming table for potentiometer and approximation errors.

3.2 Impedance waveforms of very low frequency and low frequency

In figure 7. we present one-period of sinusoidal signal, which imitate breathing action. In figure 8. distorted signal has normal noise with zero mean and relatively high variance, but does not have any high-frequency component (artifacts). Data are looped in microcontroller where we could set frequency of the signal and number of repetitions.

Simulated impedance changes causes by cardiac action with breathing component are presented in figure 9. For that kind of signals (Fig. 10. and 11.) there are also the same kind of plots as shown in figures 7. and 8.

The error analyses concerns only the theoretical error between desired waveform and that which can be produced by the designed circuit. Other sources of errors, like that from supply and passive elements could be of much greater importance, however there are not dealt with presently.

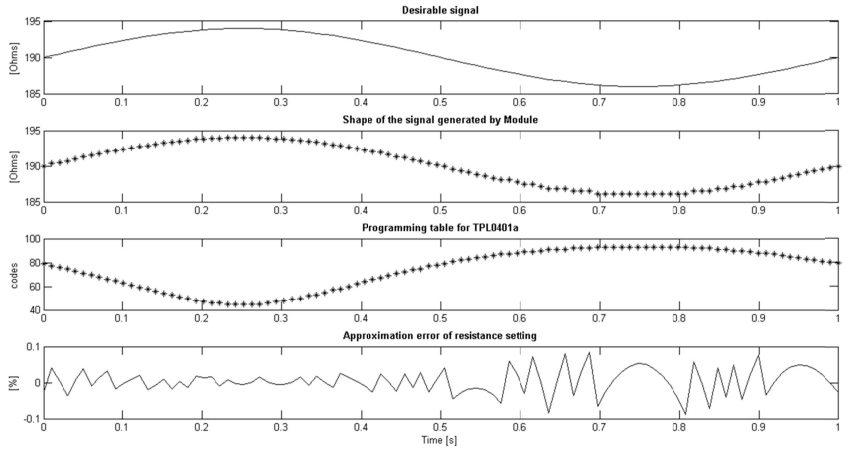

Figure 7. Application results for $f(t) = 190\Omega + 4\Omega \cdot \sin(2\pi \cdot 1Hz \cdot t)$

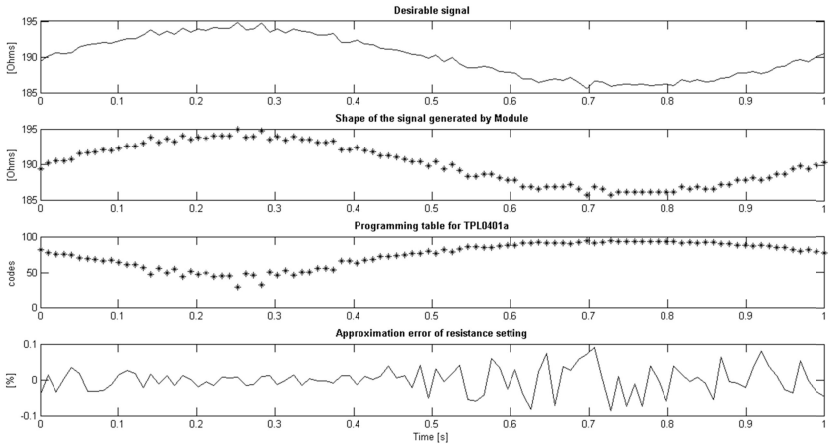

Figure 8. Application results for $f(t) = 190\Omega + 4\Omega \cdot \sin(2\pi \cdot 1Hz \cdot t) + Noise{\sim}N\left(0, \frac{1}{3}\right)$

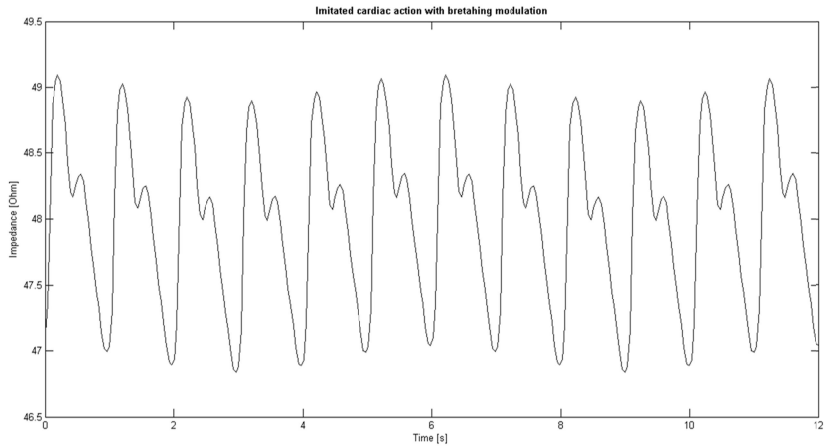

Figure 9. Imitated impedance changes caused by cardiac action with breathing modulation; $f(t) = "Cardiac\ Signal"$

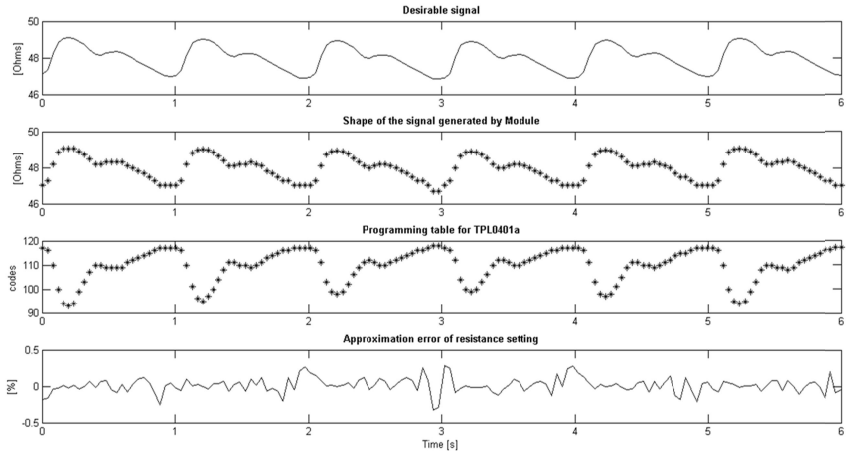

Figure 10. Application results for $f(t) = "Cardiac\ Signal"$

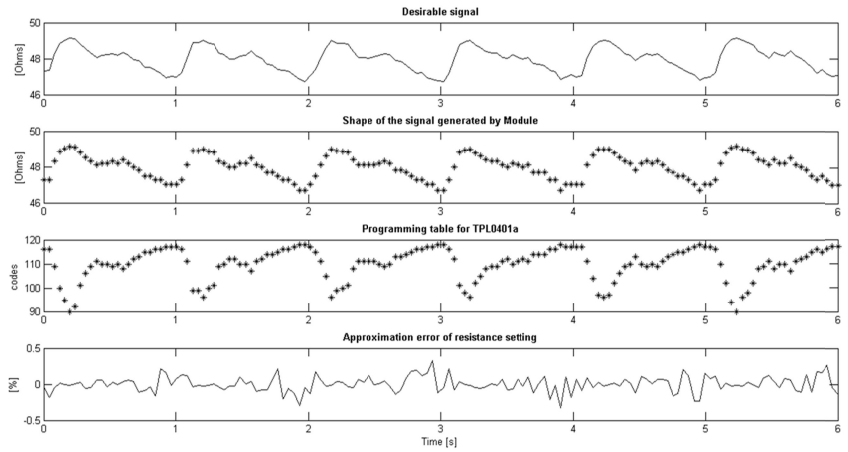

Figure 11. Application results for $f(t) = "Cardiac\ Signal" + Noise \sim N\left(0, \frac{1}{10}\right)$

4. RESULTS

Artificial Patient was used to produce variable tissue impedances and universal bioimpedance measuring device was used to measure these impedance changes. In the figure 12. we showed two readings of tissue impedance measured in Artificial Patient. Upper trace shows very-low-frequency changes of tissue impedance simulating breathing action, whereas lower trace consists low-frequency cardiac activity simulation with breathing modulation.

We have also tested an excitation current by checking the shape and amplitude after passing high electrode-skin interface impedances. Using those results we have adjusted parameters of the device: current amplitude and receiver part settings and we have chosen two working modes: "cardiac" and "respiratory", which have different amplifications.

Blue lines connect to raw signal, red ones are approximation of the local mean value of the signal fitted using low-pass filtering.

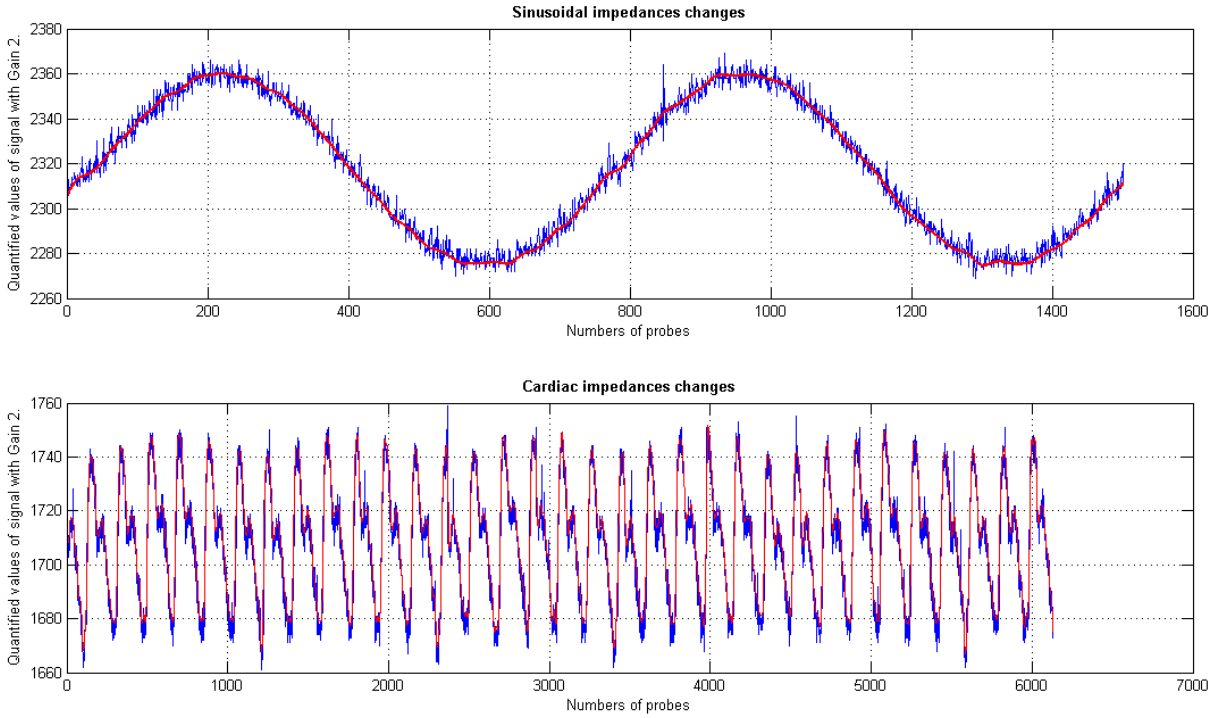

Figure 12. Reography output signal for sinusoidal and cardiac impedance changes

For the impedance changes there are distortions coming from an inaccuracy of the resistance setting, noises of the receiver part and analog-to-digital conversion. The standard deviation of the difference between the measured impedance and the reference was $\sigma(Z) \approx 0.1826\Omega$. In comparison to the measured basic impedance of 196Ω, the σ at this level (< 0.1%) seems to be negligible.

5. CONCLUSIONS

Artificial Patient can imitate impedance changes observed in man. We could program various waveforms of impedance changes which relate to heart or lungs influence on thoracic impedance. We believe that the Artificial Patient may be used to verify and calibrate various bioimpedance measuring devices by using reference signals of different characteristics chosen by operator.

REFERENCES

[1] Cybulski, G., [Ambulatory Impedance Cardiography. The Systems and their Applications.], Series: Lecture Notes in Electrical Engineering, Vol. 76, 1st Edition, Springer-Verlag Berlin and Heidelberg GmbH & Co. KG (2011)

[2] Vuorela, T., Seppa, V.P., Vanhala, J. and Hyttinen, J., "Design and Implementation of a Portable Long-Term Physiological Signal Recorder", IEEE Transactions on Information Technology and Biomedicine 14(3), 718-725 (2010)

[3] Seppa, V.P., Viik, J. and Hyttinen, J., "Assessment of Pulmonary Flow Using Impedance Pneumography", IEEE Transactions on Biomedical Engineering 57(9), 2277-2285 (2010)

[4] Młyńczak, M. and Cybulski, G., "Impedance pneumography – is it possible?", Proc. of SPIE 8454,84541T, 1-14 (2012)
[5] Spach, M.S., Barr, R.C., Havstad J.W. and Croft Long, E., "Skin-Electrode Impedance and Its Effect on Recording Cardiac Potentials", Circulation 34, 649-656 (1966)
[6] Rosell, J., Colominas, J., Riu, P., Pallas-Areny, R. and Webster, J.G., "Skin Impedance From 1 Hz to 1 MHz", IEEE Transactions on Biomedical Engineering 35(8), 649-651 (1988)
[7] Kaczmarek, K.A. and Webster J.G., "Voltage-Current Characteristics of the Electrotactile Skin-Electrode Interface", IEEE Engineering in Medicine & Biology Society 11th Conference, 1526-1527 (1989)
[8] Assambo, C. and Burke, M.J., "Low-Frequency Response and the Skin-Electrode Interface" in Millis, R., [Dry-Electrode Electrocardiography, Advances in Electrocardiograms - Methods and Analysis], InTech (2012)
[9] Medrano, G., Ubl, A., Zimmermann, N., Gries, T. and Leonhardt, S., "Skin Electrode Impedance of Textile Electrodes for Bioimpedance Spectroscopy", IFMBE Proc. 17, 260-263 (2007)
[10] Assambo, C., Baba, A., Dozio, R. and Burke, M.J., "Determination of the Parameters of the Skin-Electrode Impedance Model for ECG Measurement", Proc. of 6th WSEAS Int. Conf. on Electronics, Hardware, Wireless and Optical Communications, 90-95 (2007)
[11] Yamamoto, Y. and Yamamoto, T., "Characteristics of skin admittance for dry electrodes and the measurement of skin moisturisation", IFMBE Medical & Biological Engineering & Computing, 71-77 (1986)
[12] Dozio, R., Baba, A., Assambo, C. and Burke, M.J., "Time Based Measurement of the Impedance of the Skin-Electrode Interface for Dry Electrode ECG Recording", Proc. of the 29th Conf. of the IEEE EMBS, 5001-5004 (2007)